


Summer 8-31-2014

Investigating Propargyl-Linked Antifolates in Inhibiting Bacterial and Fungal Dihydrofolate Reductase

Joshua Andrade

University of Connecticut - Storrs, andrade.joshua.david@gmail.com

Follow this and additional works at: https://opencommons.uconn.edu/srhonors_theses

 Part of the [Enzymes and Coenzymes Commons](#), [Medicinal and Pharmaceutical Chemistry Commons](#), [Molecular Biology Commons](#), and the [Pharmaceutical Preparations Commons](#)

Recommended Citation

Andrade, Joshua, "Investigating Propargyl-Linked Antifolates in Inhibiting Bacterial and Fungal Dihydrofolate Reductase" (2014). *Honors Scholar Theses*. 399.
https://opencommons.uconn.edu/srhonors_theses/399

*Investigating Propargyl-Linked Antifolates in Inhibiting Bacterial and Fungal
Dihydrofolate Reductase*

Honors Thesis

Presented by

Joshua David Andrade

Department of Molecular and Cell Biology

University of Connecticut

2014

Abstract

Antimicrobial agents have been invaluable in reducing illness and death associated with bacterial infection. However, over time, bacteria have evolved resistance to all major drug classes as a result of selective pressure. The advancement of new drug compounds is therefore vital. The Anderson-Wright Lab has focused on developing potent and selective inhibitors of dihydrofolate reductase (DHFR), an enzyme key in cell proliferation and survival, in several pathogenic species. The lab has found that a set of compounds, known as propargyl-linked antifolates, are DHFR inhibitors that are both biologically effective and have strong pharmacokinetic properties.

The efficacy of novel propargyl-linked antifolates in inhibiting DHFR was tested with enzymatic assays in three species: *Candida albicans*, *Candida glabrata*, and *Klebsiella pneumoniae*. In order to gauge the potency of the novel compounds, the results of the tests were referenced against assay results using trimethoprim, which is a known, powerful inhibitor of DHFR. Additionally, x-ray crystallography was employed to generate a three dimensional representation of inhibitor:pathogen DHFR interactions. The data from the enzymatic assay and x-ray crystallography were utilized to deduce the structural analogs of the propargyl-linked antifolates most effective in inhibiting DHFR in the given pathogens. Knowing what specific molecular features comprise an effective inhibitor allows the lab to strive towards more ideal drug compounds and allow for future development of increasingly powerful antimicrobials.

Acknowledgements

This work would not have been possible without the help from the following institutions and individuals: Dr. Amy Anderson for introducing me to medicinal chemistry, structure based design, and mentoring me throughout this research project; Dr. Victoria Robinson for guiding my research interests and supporting my academic experience; Michael Lombardo and Janet Paulsen for helping me develop laboratory techniques and research design methods; the John and Valerie Rowe Health Professions Program for funding my research endeavors; the UConn Department of Molecular and Cell Biology and Department of Pharmaceutical Studies for allowing me access to outstanding facilities and opportunities; and the UConn Honors Program for enhancing my undergraduate education.

Antimicrobial agents have been invaluable in reducing illness and death associated with bacterial infection. However, over time bacteria have evolved resistance to all major drug classes as a result of selective pressure ^[1,2]. With current drug therapies becoming increasingly ineffective, bacterial resistance has become a threat to global health ^[3]. The advancement of new, potent antimicrobials, therefore, are vital.

The diagram illustrates the biosynthesis of purine nucleotides, showing the conversion of dietary folate to N^5,N^{10} -methylene THF and its subsequent use in the synthesis of deoxythymidine monophosphate (dTMP) and deoxyuridine monophosphate (dUMP).

Diet: Folate (vitamin B_9) is converted to N^5,N^{10} -methylene THF by the enzyme **Dihydrofolate Reductase (DHFR)**, using H^+ and NADPH as cofactors.

Intermediate: N^5,N^{10} -methylene THF is converted to N^5,N^{10} -methyl THF by the enzyme **N^5,N^{10} -Methylene-THF Reductase**, using N^5,N^{10} -Methylene-THF as a cofactor.

Final Product: N^5,N^{10} -methyl THF is converted to N^5,N^{10} -methyl THF by the enzyme **N^5,N^{10} -Methyl-THF Reductase**, using N^5,N^{10} -Methyl-THF as a cofactor.

Enzymes and Cofactors:

- Dihydrofolate Reductase (DHFR):** Converts Folate (vitamin B_9) to N^5,N^{10} -methylene THF.
- N^5,N^{10} -Methylene-THF Reductase:** Converts N^5,N^{10} -methylene THF to N^5,N^{10} -methyl THF.
- N^5,N^{10} -Methyl-THF Reductase:** Converts N^5,N^{10} -methyl THF to N^5,N^{10} -methyl THF.

Chemical Structures:

- Folate (vitamin B_9):** A purine ring system with a p-aminobenzoyl group and a p-aminobenzoate group.
- N^5,N^{10} -methylene THF:** A tetrahydrofolate derivative with a methylene group between the N^5 and N^{10} positions.
- N^5,N^{10} -methyl THF:** A tetrahydrofolate derivative with a methyl group between the N^5 and N^{10} positions.
- N^5,N^{10} -methyl THF:** A tetrahydrofolate derivative with a methyl group between the N^5 and N^{10} positions.

Enzymes and Cofactors:

- Dihydrofolate Reductase (DHFR):** Converts Folate (vitamin B_9) to N^5,N^{10} -methylene THF.
- N^5,N^{10} -Methylene-THF Reductase:** Converts N^5,N^{10} -methylene THF to N^5,N^{10} -methyl THF.
- N^5,N^{10} -Methyl-THF Reductase:** Converts N^5,N^{10} -methyl THF to N^5,N^{10} -methyl THF.

Chemical Structures:

- Folate (vitamin B_9):** A purine ring system with a p-aminobenzoyl group and a p-aminobenzoate group.
- N^5,N^{10} -methylene THF:** A tetrahydrofolate derivative with a methylene group between the N^5 and N^{10} positions.
- N^5,N^{10} -methyl THF:** A tetrahydrofolate derivative with a methyl group between the N^5 and N^{10} positions.
- N^5,N^{10} -methyl THF:** A tetrahydrofolate derivative with a methyl group between the N^5 and N^{10} positions.

Figure 1. Folate Biosynthetic Pathway. The primary folate biosynthetic pathway is highlighted in yellow. De novo synthesis of dihydrofolate in bacteria is represented in green. Key products of the reaction are shown in blue ^[6].

When the pathway becomes inhibited, the purines and amino acids are not effectively synthesized, dTMP production is halted, and consequently, there is no DNA replication or cell proliferation. In this way, folate pathway inhibitors, or antifolates, have become a popular area of drug design and optimization ^[4]. One effective target for inhibitors is an integral enzyme in the pathway, dihydrofolate reductase (DHFR). DHFR converts dihydrofolate to tetrahydrofolate (THF). As DHFR is the sole source of THF, which has been described as a necessary precursor for the synthesis of vital cellular components, blocking DHFR's activity will halt the target cell's growth. Further, beyond its ability to impact cellular proliferation, DHFR is an optimal target because it is a widely conserved enzyme, present in many bacterial and eukaryotic organisms. Because of this, DHFR inhibitors may be used in treatment for numerous pathogenic species. At the same time, there are differences between the amino acid sequence in pathogen and human DHFR which allows for selectivity ^[5]. It is also one of the best studied enzymes in the folate pathway. Structural models exhibiting the inhibitor:enzyme interaction of DHFR are widely available and information on DHFR mechanism of action and resistance is vast. This provides researchers insight on how to improve upon novel drug compounds ^[6].

One widely used DHFR inhibitor is trimethoprim. It is a very effective 5-substituted-2,4-diaminopyridine clinically used compound. In fact, it binds bacterial DHFR 10^5 times more tightly than it does vertebrate DHFR ^[6]. However, resistance tends to develop against this drug in a few ways. In Gram positive organisms, point mutations in the DHFR enzyme, which affects

the ability of the drug and enzyme to bind, have been described. In Gram negative bacteria, bypass enzymes, spread by mobile genetic elements, are the primary cause of resistance ^[6]. Again, with the emerging resistance, new drug discovery is crucial. As TMP is safe and clinically effective when resistance has not been established, research on how to optimize this DHFR inhibitor has honed in on trimethoprim's structure, specifically its diaminopyridine ring. Drugs improve upon TMP by modifying the diaminopyridine ring in a way that, for example, may allow it to bind the DHFR enzyme more tightly or give it either a broad or particularly focused spectrum activity ^[6].

The Anderson-Wright Lab has focused on the development of propargyl-linked antifolates. These compounds contain the diaminopyridine moiety linked with a propargyl group to a variable hydrophobic functional domain ^[7].

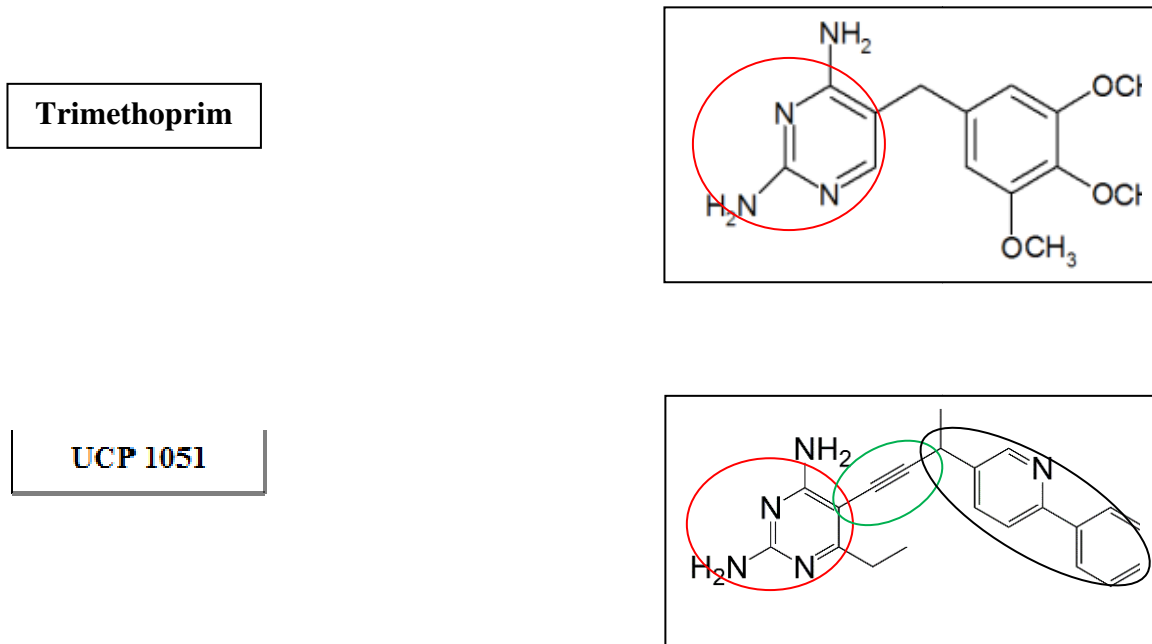


Figure 2. Trimethoprim and UCP 1051, a novel propargyl-linked antifolate synthesized by the Anderson-Wright Lab, have the same diaminopyridine moiety (red). Also pictured in UCP 1051

is the propargyl-linker (green) and the hydrophobic domain, which varies between drug compounds (black).

Crystal structures of the inhibitor:enzyme interaction in several pathogens indicate that the propargyl-linker occupies a space in the DHFR that bridges two critical pockets in its active site. One pocket interacts with the diaminopyridine moiety while the other site is hydrophobic, interacting with the variable hydrophobic domain. Over the course of iterative cycles of structure based drug design, adding a biphenyl moiety to the hydrophobic region of the propargyl-linked antifolate was a potent lead against numerous prokaryotic and eukaryotic organisms. Moreover, these compounds displayed strong selectivity. For instance, the propargyl-linked antifolates with the biphenyl moiety showed a 2350-fold greater potency for DHFR in *Candida glabrata* over human DHFR ^[6]. The advancement of propargyl-linked antifolates was taken a step further as a series of compounds containing nitrogeneous heterocyclic moieties were synthesized in an effort to increase the hydrophobicity, and thus, the solubility of the drug. The heterocyclic compounds exhibited superior activity against several species.

Improvement upon the propargyl-linked antifolate design is sought after by the lab. There is still opportunity for drug compounds to be more potent, selective, and efficacious in inhibiting the DHFR enzyme. The antifolate design is advanced by running several sets of tests on a variety of analogs. Observing what structural themes allow for drug potency gives researchers the ability to gauge what comprises an ideal inhibitor. One test that is often used is an enzymatic assay. In this test, the DHFR is combined *in vitro* with its substrate, a cofactor, and other essential chemicals that allow the conversion of dihydrofolate to tetrahydrofolate. The reaction rate is measured and recorded. The process is repeated in later trials, but an inhibitor is added to the

enzyme. The reaction rates of the trials using inhibitors are compared to the trial that did not have the inhibitor present. The assay examines how much of the drug is needed to inhibit the enzyme 50 percent of its typical action. Assay results allow for optimization around potential leads. In cycles of development, this will generate a compound with an outstanding structure which makes is tremendously potent. Equally important to drug discovery is x-ray crystallography, which gives a three dimensional representation of the inhibitor interacting with the enzyme. By visualizing the molecular interactions, the researcher can make fine adjustments to the drug's structure that will make it more powerful. Three microorganisms that the lab has involved in enzymatic assays and crystallography are *Candida glabrata*, *Candida albicans*, and *Klebsiella pneumoniae*.

Candida infections are nosocomial diseases in that they typically occur during a stay within a hospital setting ^[8]. This is a result of the species thriving on and being prevalent within critically ill and immunocompromised patients. Old age, major surgery, premature birth, AIDS, use of catheters, and chemotherapy are only some of the factors that contribute to a deficient immune system and an increased susceptibility to invasive candidiasis ^[9,10]. *Candida* proves to be a cause for concern as the frequency of *Candida* in blood cultures in US hospitals rose 52% over just a three year period ^[8]. Combined with the fact that it has a forty percent mortality rate in infected hospitalized patients ^[11], *Candida* infections are especially dangerous. Since there are no licensed vaccines available for the treatment of *Candida* ^[11], certainly, the need for the development of therapeutic drug compounds is evident.

Two of the most commonly used antifungal agents, or antimycotics, are azoles and polyenes. Azoles and polyenes interact with ergosterol, a major component of the *Candida* cellular membrane. When the ergosterol is impacted by the compounds, the membrane does form

properly, and the cell is unable to function. Polyenes bind ergosterol directly and alter membrane fluidity. Azoles have a different method of action as they inhibit Cyp51, which catalyzes the formation of ergosterol ^[12]. *C. glabrata*, however, exhibits strong resistance to both of the compounds. The resistance of *C. glabrata* to polyenes is the result of the organism developing changes in its membrane structure that prevent the drugs necessary interaction with the membrane. Regarding azoles, *Candida* has garnered multidrug resistance by increasing its expression of drug efflux pumps ^[11]. The resistance to azoles has been particularly alarming. Of all the *Candida* strains, *C. glabrata* is the most resistant to some of the most commonly prescribed azole drug classes, itraconazole and fluconazole ^[13]. Also, there was a 1.9% *C. glabrata* resistance to fluconazole in 2002 that spiked to 17.1% in 2006 ^[14]. As the resistance to current drug compounds continually rise, the development of novel compounds with distinct mechanisms of action become increasingly important.

Candida albicans, the candida species that most commonly causes fungal infections within hospitals, garners resistance in multiple mechanisms. Much like *C. glabrata*, *C. albicans* resistant organisms have been observed to increase their expression of efflux pumps. But, the most common mechanism is based on the alteration of the target enzyme of the ergosterol biosynthesis pathway, sterol 14 alpha demethylase, which is encoded by the *ERG 11* gene. Resistance develops by the increased expression of *ERG11*, increasing the intracellular pool of sterol 14alpha demethylase, which then increases the effective drug dose. Moreover, point mutations in gene lead to an alteration of amino acid residues and spatial configuration. The azole drugs may no longer bind to the enzyme with the same affinity, and thus, are much less potent ^[15].

Klebsiella pneumoniae is the most clinically important member of the *Klebsiella* genus of *Enterobacteriaceae*. It has been noted as a common pathogen for nosocomial pneumonia, septicemia, and wound infections. *K. pneumoniae* has also been isolated in more uncommon infections like endocarditis, cholecystitis, peritonitis, meningitis, and pyomyositis. Beta-lactam antibiotics are typically prescribed to treat *K. pneumoniae* infections. Historically, they have been one of the most effective drug classes in inhibiting bacterial growth. β -Lactams exert their antibiotic effects by mimicking the natural D-Ala-D-Ala substrate of the family of enzymes known as penicillin-binding proteins (PBP), which are responsible for cross-linking the peptidoglycan component of the bacterial cell wall. The integrity of the bacteria cell wall becomes compromised when this process is inhibited, and the cell lyses ^[19].

However, constitutive use of beta-lactams to combat *K. pneumoniae* has led to the bacteria evolving resistance, producing mutations and strong expression of beta-lactamases. The bacteria may even express beta-lactamase activity against newly developed beta-lactam antibiotics. These are referred to as extended spectrum beta-lactamases (ESBLs). Carbapenem antibiotics, beta-lactams that have a structure which make them resistant to lactamases, have been used to treat any serious infection caused by ESBLs. Nevertheless, *K. pneumoniae* has developed resistance to these drug compounds via a novel mechanisms referred to as *Klebsiella pneumoniae* carbapenemases (KPCs) ^[16]. KPCs are a particular cause for concern as KPC-producing organisms can confer resistance to numerous drug classes such as fluoroquinolones and aminoglycosides, in addition to beta-lactams. Because of this, infections due to KPCs are associated with poor therapeutic treatment and mortality rates up to 50%. With the limited number of drug compounds available to eliminate KPCs, novel structures that are biologically effective are invaluable ^[17].

Materials and Methods

Protein Expression

Escherichia coli were transformed by *C. glabrata* dihydrofolate reductase (CgDHFR) and *C. albicans* dihydrofolate reductase (CaDHFR) DNA. After cultures of the *E. coli* were grown, expression of the DHFR protein was induced by the addition of β -D-thiogalactoside. The culture was centrifuged so *E. coli* cells only, which at this point contained the DHFR, were easily extracted from the culture. The cells were then lysed by Bug Buster, a reagent that breaks open *E. coli* cell walls, and further centrifuged. The supernatant was exposed to ammonium sulfate precipitate which eliminated many proteins, but left the desired enzyme. The protein was further purified with use of a methotrexate column. In this, the DHFR was bound to the column while other non-desired proteins and cellular contents diffused through. Thereafter, the column, which still held the DHFR, was washed with dihydrofolate. The DHFR could then diffuse from the column, and be collected. The DHFR was flash frozen and stored at -80 °C until further use.

Crystallography

The purified DHFR was incubated with an enzyme cofactor, NADPH, and UCP111H (Figure 12). A Linbro plate was filled with varying amounts of salt, PEG precipitant, water, and differing pH buffer in each of the 24 wells that comprise the plate. The contents of these wells promote the formation of a crystal via the hanging drop diffusion method. In this, a 2 μ L drop of the DHFR infused with the drug was be combined with a 2 μ L drop of precipitant and placed on a coverslip. This coverslip was sealed to the top of one of the wells with the aid of high vacuum grease. After sitting at 4°C for two weeks, the precipitant vaporized and transferred into the

reservoir of the well until the system reached equilibrium. At this point, conditions were optimal for protein crystallization^[18]. Protein crystals were extracted and flash frozen for preservation.

After, the crystals were shot with an X-ray. These X-rays generated a diffraction pattern which was processed to give information about the structure and electron density of the protein infused with the drug compound. Several programs including Phaser, COOT, and Refmac 5 were utilized in order to create a three dimensional representation of the protein and inhibitor based on the collected diffraction pattern.

Enzymatic Assay

An assay buffer consisting of 20mM TES, 50 mM KCl, 0.5mM EDTA, 10mM beta-mercaptoethanol, and 1mg/ml of BSA was prepared. One mg/mL of *K. pneumoniae* A1 DHFR, 20 mM NADPH, and 1mM dihydrofolate were also prepared. The enzyme activity assay was performed by monitoring the rate of NADPH consumption at 340nm over the course of 5 minutes. Reaction were performed with the assay buffer, NADPH cofactor, the dihydrofolate substrate, and the pure enzyme. The reactions were performed in triplicate.

Results

K. pneumoniae A1 DHFR

Drug Compound	Average IC50 (μM)	Std Deviation
TMP	20.166	1.69
UCP 1098	0.438	0.0349
UCP 1099	1.716	0.2745
UCP 1101	2.319	0.0148
UCP 1097	2.376	0.4532
UCP 1093	4.221	0.3852
UCP 1051	17.553	1.8193
UCP 1092	25.437	1.617
UCP 1100	65.239	1.5339

Figure 3. IC50 values for *Klebsiella pneumoniae* A1 DHFR interacting with differing novel propargyl-linked antifolates synthesized by the UConn Pharmacy Anderson-Wright Laboratory.

Reactions were run in triplicate and standardized.

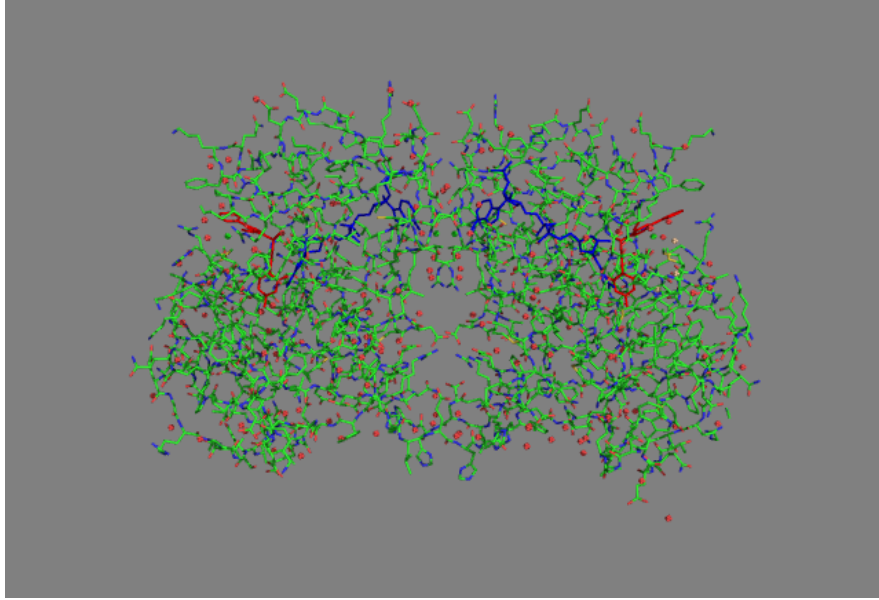


Figure 4. *Candida glabrata* dihydrofolate reductase complexed with NADPH (blue) and UCP 111H (red).



Figure 5. Quaternary structure of *Candida glabrata* DHFR. There are 6 alpha helices (red) and 13 beta sheets (yellow) in the respective homodimers.

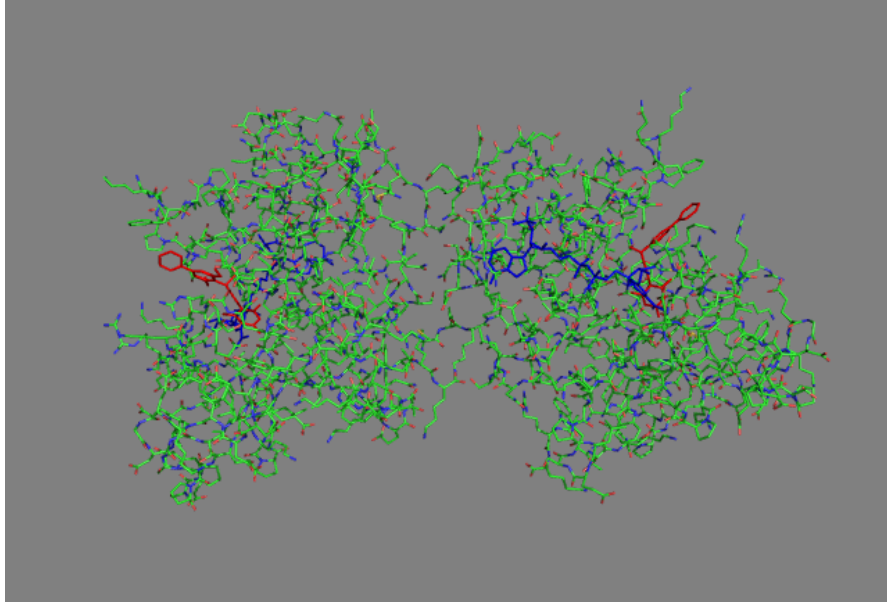


Figure 6. *Candida albicans* dihydrofolate reductase complexed with NADPH (blue) and UCP 111H (red).

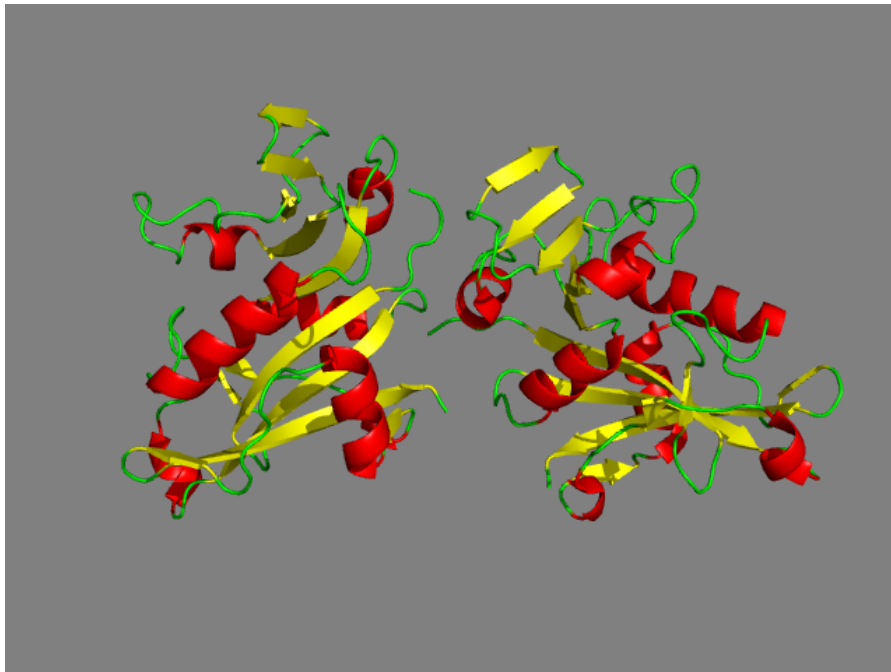


Figure 7. Quaternary structure of *Candida albicans* dihydrofolate reductase. Both homodimers consists of 11 sheets (yellow) and 7 helices (red).

***K. pneumoniae* A1 DHFR Enzymatic Assay:** The *Klebsiella pneumoniae* A1 DHFR has a different structural conformation than wild type *K. pneumoniae* DHFR. As a result, drug compounds bind the wild type DHFR and A1 DHFR differently. This is clearly seen in trimethoprim, to which the A1 DHFR has become resistant. The data reflects that TMP has a high IC₅₀ value for A1 DHFR. An IC₅₀ is a measure of what concentration of an inhibitor is needed to inhibit the enzyme fifty percent. Thus, the greater amount of drug needed for inhibition, the less potent it is. The IC₅₀ value of 20.166 μ M seen in A1 DHFR, as compared to 0.106 μ M in wild type *K. pneumoniae* DHFR, suggests that TMP binds much less tightly and is less effective against the A1 DHFR.

In the IC₅₀ values recorded, the drug compounds may essentially be divided based on their efficacy. UCP 1098 is extremely effective in inhibiting A1 DHFR while the next set of compounds, UCP 1099, 1101 and 1097 show less potency, but still are decent in inhibiting the enzyme. A slight drop in efficacy is seen with UCP 1093, and then, the remaining compounds tested; UCP 1051, 1092, and 1100 are particularly ineffective in inhibiting the A1 DHFR.

***CaDHFR and CgDHFR* crystallization:** High quality, homogeneous material is desired for a satisfactory diffraction pattern. The first step is obtaining quality crystals. As stated before, UCP 111H was incubated with either CaDHFR or CgDHFR and crystallized. A trial and error method was employed in order to determine what conditions and chemicals were needed to grow quality crystals. Initially, a wide range of concentrations and types of salt, precipitant, and buffers would be placed in the Linbro wells. After incubating for nearly two weeks, the following would be observed in the wells: nothing, precipitation, or small crystals. The latter would be considered a “hit,” but these crystals would be either too small to obtain a good diffraction pattern or would be

impure. Researchers optimized around the conditions in the hits, making minute adjustments, until they found what best facilitated large, uniform, crystal growth. The conditions that best enabled both the CaDHFR and CgDHFR crystal growth in the Linbro wells were: 0.1M Tris Base pH between 8-8.75, varying amounts of magnesium chloride between 10 and 100 μ L, PEG 4000 precipitant 30% w/v between 300 and 350 μ L, and the remainder of the 500 μ L well was filled with water. Also, other techniques that were used to determine what led to quality crystal growth were altering the protein concentration, temperature of incubation, and seeding.

The crystal was mounted in a beam, which generates and projects an x-ray wavelength, and onto a device that rotates so the ray may strike it at different angles. After the crystals were shot with the ray, a diffraction pattern was obtained. In this experiment, powerful synchrotrons at Brookhaven National Laboratory were used. These machines shoot a very intense x-ray beam with high quality optics, allowing for a high signal to noise ratio in the diffraction pattern. This, in turn, leads to a better three dimensional representation of the macromolecule ^[18]. Once the pattern had been obtained, researchers needed to ensure that the resolution was sufficient to make accurate structure determination. Also, the unit cell dimensions, the crystal system, and the space group was analyzed.

When the pattern had been successfully captured, this data was processed with several programs with algorithms to calculate an electron density map. The map forms the contours into which the protein structure will be built. The quality of the map is improved through refinement programs until it may no longer be enhanced. From this, the model may be uploaded to the Protein Data Bank and viewed as a PDB file. PyMOL was the molecular visualization system used to view the PDB files as seen in Figures 4-7.

Discussion and Conclusion

The purpose of conducting the various tests in the experimental procedures were to discover what propargyl-linked antifolate structural analogs best inhibit dihydrofolate reductase action in *C. albicans*, *C. glabrata*, and *K. pneumoniae*. Observing what analogs best inhibit the enzyme can assist in the generation of more potent drug compounds in iterative cycles of antifolate development.

C. albicans and *C. glabrata* were explored through x-ray crystallography. This gave a three dimensional representation of the molecular structure of DHFR complexed with a given drug compound. In this procedure, the enzyme was infused with UCP 111H.

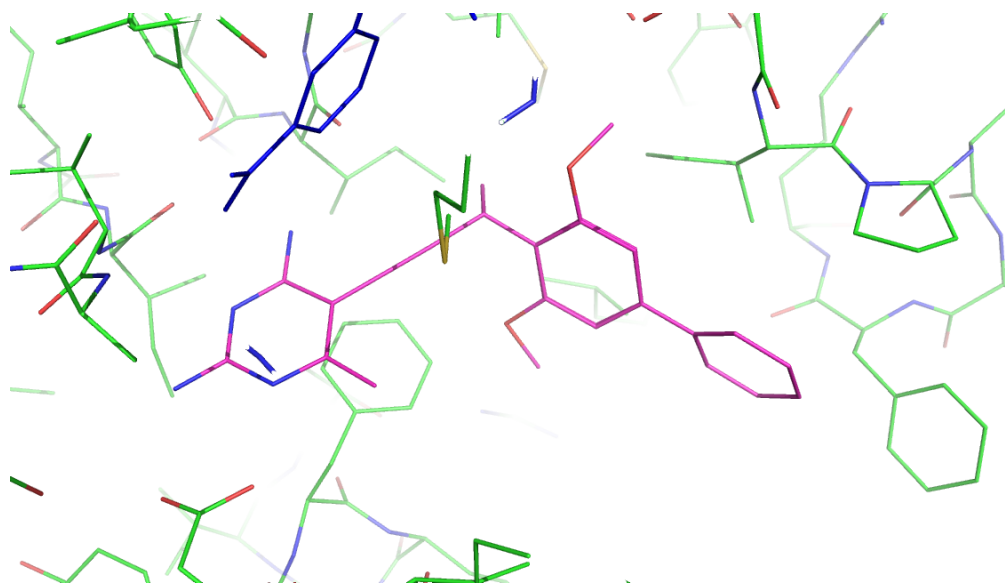


Figure 8. Pictured is UCP 111H in the active site of *C. albicans* DHFR. The drug compound is colored based on its chemical structure: Carbon (pink), Nitrogen (Blue) and Oxygen (Red).

When looking at the structure in Figure 8, it is clear to see that there are two distinct areas in which the drug interacts. Using PyMOL, one can find what molecules are interacting

with another by measuring the distance between two different structures. Molecules within 3.5 Å of each other are potentially interacting. First is the diaminopyridine, which interacts with several specific amino acid side chains. The 2 substituted amine in the diaminopyridine is bonded to an oxygen in glutamic acid. Glutamic acid has an electrically charged side chain. This reflects how fluctuations in pH may affect the binding of the drug compound to the enzyme. The pH will determine if hydrogen atoms remain bound to the side chain, and thus, if the side chain becomes charged. The charge on the side chain will affect how it binds to different molecules. Of course, then, it impacts how the drug compound may bind to the protein at the active site. The 4 substituted amine may be interacting with oxygens on two different isoleucine side chains. Isoleucine is a hydrophobic amino acid. The area of the drug compound that interacts with this amino acid must be hydrophobic as well. The presence of any largely polar substances will not allow for tight interaction with the protein. When the inhibitor is unable to bind tightly, the drug becomes ineffective. So, the amine must be satisfactory in binding to these hydrophobic regions.

The diaminopyridine, however, has already been noted as successfully binding to the enzyme. Thus, it is not necessarily the target of drug optimization. As noted before, the propargyl group links the drug compound to another area of the active site in DHFR. This is where advancement in the propargyl-linked antifolate design has proven key. First attached to the propargyl-linker is a methyl group. This methyl group binds with an isoleucine, again, a hydrophobic amino acid. It is invaluable to have a methyl, or another hydrophobic group, in this region because a charged molecule will be detrimental because how the antifolate binds. A methyl group is also optimal because too bulky of a hydrophobic group may lead to hinderance and prevent the compound from attaching to the site tightly.

Also bound to the propargyl is a biphenyl group with a methoxy attached to the benzene ring closest to the linker. Numerous amino acid side chains in this region of the protein are hydrophobic, and because of this, it is crucial to have a complementary hydrophobic moiety. The largely hydrophobic biphenyl serves this purpose. The methoxy binding is slightly more perplexing. It can bind with phenylalanine, or serine and threonine. This is because the biphenyl is free to rotate around a single bond it has. As it rotates, the methoxy may become attached to either the phenylalanine or both the serine and threonine. Yet, phenylalanine – hydrophobic, and threonine and serine – both polar, are very different amino acids. Perhaps having a methoxy in this region is necessary as it holds the capability to bind to both types of compounds. The oxygen provides some polarity, maybe enough to facilitate binding to the polar side chains, but it is not too polar to prevent attachment to the nonpolar phenylalanine.

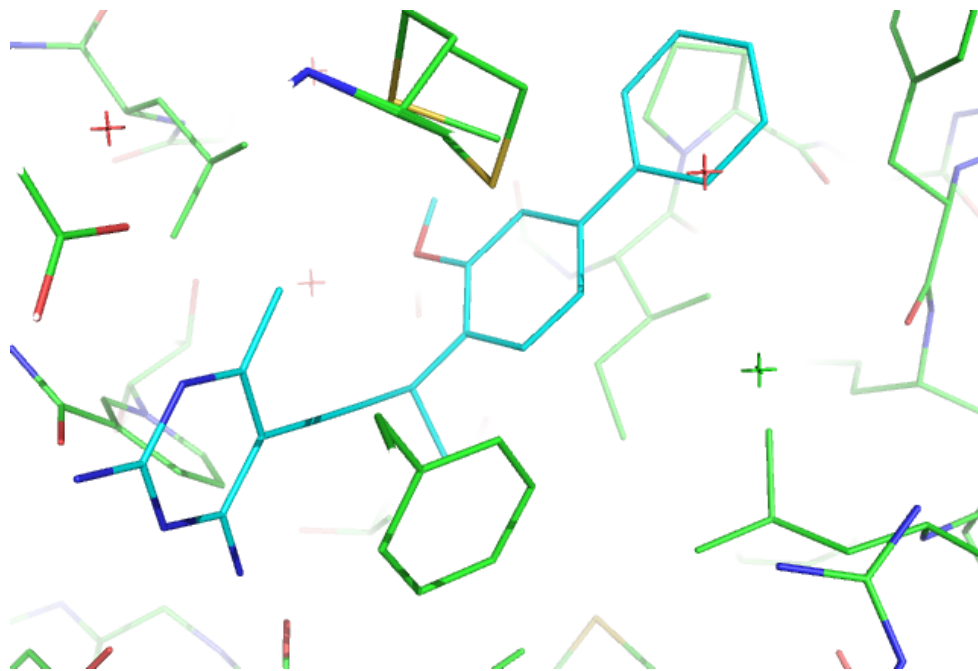


Figure 9. UCP 111H in the active site of the CgDHFR. The CgDHFR shares some key similarities and differences in binding to the drug compound as CaDHFR. The chemical structure of UCP 111H is Carbon (light blue), Nitrogen (dark blue), and Oxygen (red).

There are similarities in the interaction of the drug compound and enzyme between CaDHFR and CgDHFR. In CgDHFR, the inhibitor action may be broken up into the same two sections in the active site as CaDHFR: the diaminopyridine and the hydrophobic region. There were only few differences in what amino acids bind the inhibitor. First, the 2 substituted amine in the diaminopyridine in CgDHFR may interact with an oxygen on glutamic acid, which has been described in CaDHFR, but it also may be bonded to an oxygen on threonine. The 4 substituted amine is bonded with an isoleucine as in CaDHFR. One other difference between the two species is the action of the methyl group on the ring. In CaDHFR, the methyl was not observed to be bound to any part of the protein. Yet in CgDHFR, it is interacting with a sulfur on methionine. This adds added benefit to the drug compound as more bonds provide more opportunity for the drug to remain in the active site and a more sound inhibition.

The methoxy group attached to the biphenyl interacts with serine. It may be valuable to have a functional group in this region that binds with serine as it is a polar amino acid. With the biphenyl being largely hydrophobic, a functional group that interacts with serine may sequester it and stop it from preventing the drug's action in the hydrophobic region. The methoxy does not bind with multiple side chains as seen in CaDHFR. Numerous hydrophobic amino acids are present in the hydrophobic region of the active site that interact with the drug. Included is leucine, phenylalanine, and isoleucine. The ring in proline, also showing some hydrophobicity, interacts as well.

The IC₅₀ value for UCP 111H in *C. albicans* and *C. glabrata* were obtained by the lab. The value for UCP 111H in *C. albicans* is 0.02 µM while it is 0.0055 µM in *C. glabrata*. There is a clear difference between the two species, and it appears that UCP 111H is more effective in inhibiting the CgDHFR than CaDHFR. The differing values, of course, may be attributed to the two enzymes' varying structures. CgDHFR has a few more interactions taking place with amino acids than CaDHFR. This may be giving UCP 111H in *C. glabrata* more stability and strength.

Since both of the *Candida* species may exhibit similar symptoms in an infected patient, and it can be difficult for providers to make a diagnosis and prescribe a drug solely for *C. albicans* or *C. glabrata*. Moreover, it wastes valuable treatment time if the diagnosis is initially erroneous and the incorrect drug is given. Thus, drugs that halt both *C. albicans* and *C. glabrata* action are desired. It is advantageous that the DHFR active site is similar in both species. This allows potential for the antifolates to bind both enzymes and inhibit DHFR action, as seen in UCP 111H. Enzymatic assays and *in vitro* cell based assays would be used to measure exactly how effective the drug compounds are in the respective species.

Analysis of the *K. pneumoniae* enzymatic assay shows that some structural themes lead to potent inhibitors while others do not. First noticeable is the hydroxyl group off the propargyl-linker as opposed to a methyl group (Figure 10). The substantially higher IC₅₀ value reflects that UCP 1100 is far less potent than UCP 1093. The only aspect of their structures that differ is the highlighted methyl and hydroxyl. This suggests that a hydroxyl in this area greatly hinders the binding of the antifolate to the enzyme. This is likely because a nonpolar amino acid is close to where the methyl or hydroxyl would have to interact. The interacting amino acid may be an

isoleucine, as seen in the *Candida* species. Having a polar hydroxyl present would prevent tight bonding.

The stereochemistry of the methyl group plays a role as well. UCP 1098 and UCP 1099 (Figure 12) are identical except for the respective R and S conformations. UCP 1098 has an IC₅₀ of 0.438 μ M while UCP 1099 has an IC₅₀ of 1.716 μ M. One explanation for the difference is that the given stereochemistry may affect the distance of the methyl group to the interacting isoleucine, also affecting the strength of the bond. The disparity between the compounds is not extremely great, but the position of the methyl group is certainly worth considering in future drug design.

UCP 1092 and UCP 1101 (Figure 11) have a distinct difference in their IC₅₀ values. Nevertheless, the structures of the two compounds change only slightly. The varying potency is the cause of one, or a combination of, the following structural dissimilarities: the ethyl group present on the diaminopyridine in UCP 1101 but missing from UCP 1092; the methoxy on the benzene ring in UCP 1092 but missing from UCP 1101; the nitrogen on the benzene ring in UCP 1101, absent on UCP 1092; or the altering conformation of the heterocyclic ring attached to the benzene. In order to determine what exactly affects the antifolate's binding, a crystal structure of the *K. pneumoniae* A1 DHFR would have to be obtained. As seen in the crystal structures of CaDHFR and CgDHFR, the contributing molecular forces could be analyzed.

Another set of IC₅₀ values that contrast substantially are UCP 1093 and 1052 (Figure 12). These two compounds are entirely identical, with the exception that UCP 1093 has a heterocyclic, aromatic 5 carbon, 1 nitrogen ring in the biphenyl moiety while 1052 has an exclusively carbon ring. The IC₅₀ value for 1052 is 17.553 μ M and 1093 is 4.221 μ M. The data

suggest that the nitrogen must be interacting with a pivotal amino acid that greatly affects how the compound binds.

In all, UCP 1098 (Figure 12) is rather potent at a 0.438 μM IC₅₀. Perhaps it is the meta linked biphenyl contributes to strong bonding, or it may be the 3 carbon, 2 oxygen ring attached to the benzene ring that positively affects the inhibitor's strength. The next step in the experimental design would be to crystalize the A1 DHFR with 1098. This would allow researchers to deduce what amino acids are key in this drug's interaction. Optimization around the UCP 1098 design would give an even tighter bond to the active site and successful inhibition of the A1 DHFR.

References

1. National Research Council, Committee on Drug Use in Food Animals. *The use of drugs in food animals: benefits and risks*. Washington (DC): National Academy Press; 1999.
2. Mellon M, Benbrook C, Benbrook KL. *Hogging it: Estimates of antimicrobial abuse in livestock*. Cambridge (MA): Union of Concerned Scientists; 2001.
3. Brolund A, Sundqvist M, Kahlmeter G, Grape M (2010) Molecular Characterisation of Trimethoprim Resistance in *Escherichia coli* and *Klebsiella pneumoniae* in During a two Year Intervention on Trimethoprim Use. *PLoS One* 5(2); e9233
4. Anderson A, Wright D. Antifolate Agents: A Patent Review (2006-2010). *Expert Opin Ther Pat*. 2011 September ; 21(9): 1293–1308.
5. Lamb K, Anderson A, Wright D, G-Dayananandan N (2013) Elucidating Features That Drive the Design of Selective Antifolates Using Crystal Structures of Human Dihydrofolate Reductase. *Biochemistry*, 52, 7318-7326.
6. Zhou W, Anderson A, Wright D, Scocchera E (2013) Antifolates as effective antimicrobial agents: new generations of trimethoprim analogs *Med. Chem. Commun.*, 4, 908-915.
7. Zhou W, Anderson A, Wright D, Hill D, Viswanathan K (2012) Acetylic Linkers in Lead Compounds: A Study of the Stability of the Propargyl-Linked Antifolates. *Drug Metabolism and Disposition*, 40, 2002-2008.
8. M. Pfaller et al., Epidemiology and outcomes of candidemia in 3648 patients: data from the Prospective Antifungal Therapy (PATH Alliance®) registry, 2004–2008 *Diagnostic Microbiology and Infectious Disease*. **2012**, 1-9
9. M. Nucci, Kieren Marr, Emerging Fungal Diseases, *Clin. Infect. Dis.*, **2005**, 41, 521-526
10. R. Lewis, P Viale et al., The potential impact of antifungal drug resistance mechanisms on the host immune response to *Candida*, *Virulence*, **2012** 3:4, 368-376
11. I. Francois, A. Aerts et al., Currently Used Antimycotics: Spectrum, Mode of Action and Resistance occurrence, *Current Drug Targets* **2005**, 6, 895-207
12. Z. Kanafani et al., Resistance to Antifungal Agents, *Clin. Infect. Dis*, **2008**, 46, 120-128
13. R. Hajjeh, A. Sofair et al., Incidence of Bloodstream Infections Due to *Candida* Species and In Vitro Susceptibilities of Isolates Collected from 1998 to 2000 in a Population-Based Active Surveillance Program, *Journal of Clinical Microbiology*, **2004**, 42, 1519-1527
14. T. Chen, Y. Chen et al., Fluconazole exposure rather than clonal spreading is correlated with the emergence of *Candida glabrata* with cross-resistance to triazole antifungal agents, *Kaohsiung Journal of Medical Sciences*, **2012**, 28, 306-315
15. Strzelczyk J, Slempek-Migiel A, Rother M, et al., Nucleotide substitutions in the *Candida albicans* ERG 11 gene of azole-susceptible and azole-resistant clinical isolates. *Biochimica Polonica*, **2013**, 60, 547-552.

16. Jadhav S, et al., Increasing incidence of multidrug resistance *Klebsiella pneumoniae* infections in hospital and community settings. *International Journal of Microbiology Research*, **2012**, 4, 253-257.
17. Lee GC, Burgess DS., Treatment of *Klebsiella pneumoniae* Carbapenemase (KPC) infections: a review of published case series and case reports. *Analysis of Clinical Microbiology and Antimicrobials*, **2012**, 11:32, <http://www.ann-clinmicrob.com/content/11/1/32>
18. M.S. Smyth, J. Martin, x Ray Crystallography, *J Clin Pathol:Mol Pathol* **2000**, 53, 8–14
19. Worthington R., Melander C., *J Org Chem*. May 3, 2013; 78(9): 4207–4213.

Figures

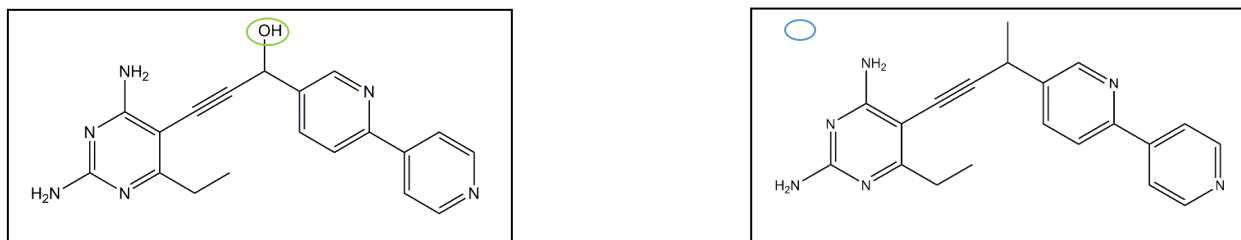


Figure 10. UCP 1100 (left) has an IC₅₀ value of 65.239 μ M while UCP 1093 (right) has an IC₅₀ value of 4.221 μ M.

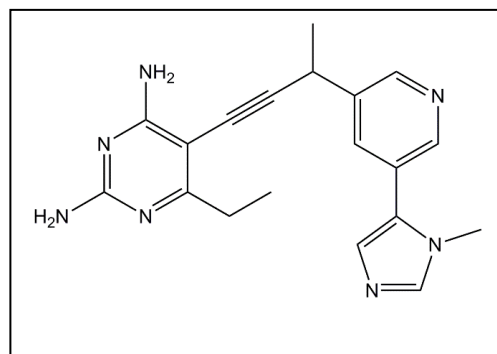
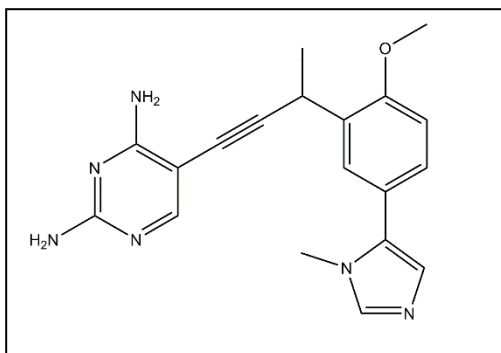
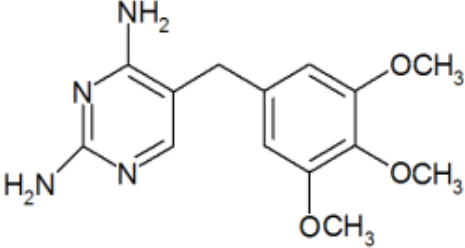
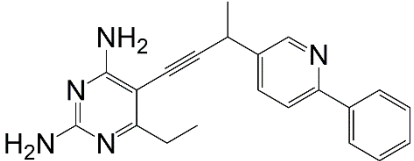
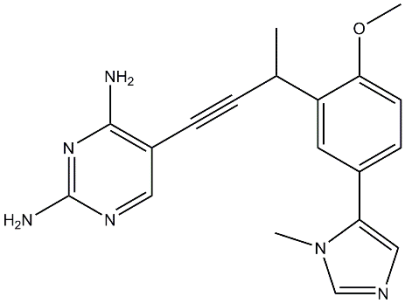
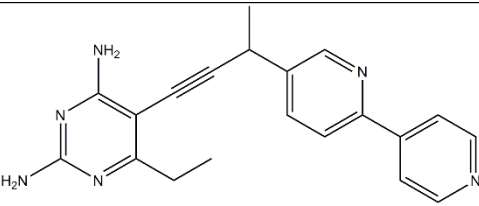
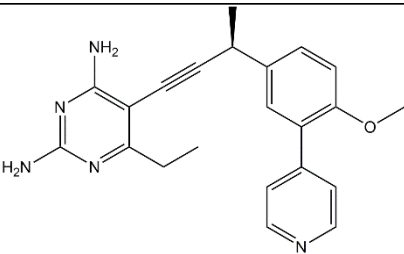
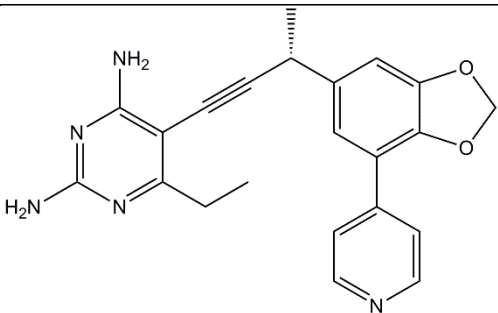
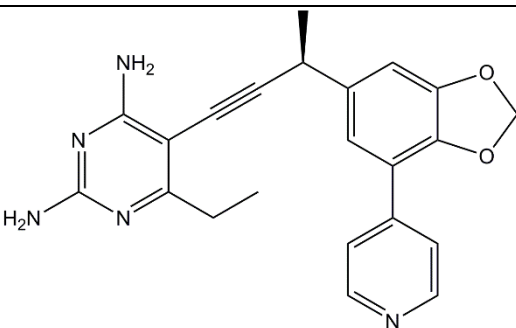


Figure 11. UCP 1092 (left) has an IC₅₀ value of 25.437 μ M and UCP 1101 (right) has an IC₅₀ of 2.319 μ M. Highlighted in UCP 1101 are functional groups that differ from UCP 1092

<i>Drug Compound</i>	<i>Structure</i>
Trimethoprim	
UCP 1051	

UCP 1092	
UCP 1093	
UCP 1097	
UCP 1098	
UCP 1099	

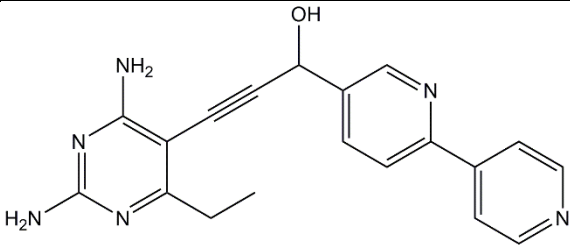
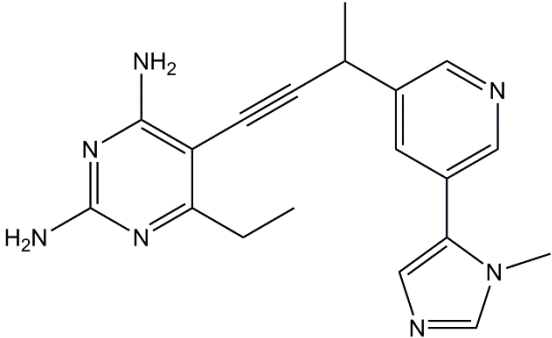
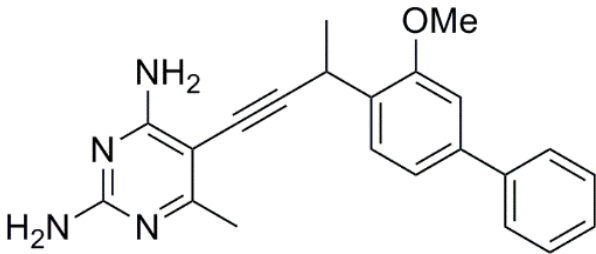
UCP 1100	
UCP 1101	
UCP 111 H	

Figure 12. Displayed are the names and structures

structures of the drug compounds utilized in the enzymatic assay of *K. pneumoniae* and crystallography of the *Candida* species.

